

Geometric properties of the first singlet S-wave excited state of two-electron atoms near the critical nuclear charge

Tong Chen(陈彤), Sanjiang Yang(杨三江), Wanping Zhou(周挽平), Xuesong Mei(梅雪松), and Haoxue Qiao(乔豪学)

Citation: Chin. Phys. B, 2024, 33 (**10**): 103101. DOI: 10.1088/1674-1056/ad6422
Journal homepage: http://cpb.iphy.ac.cn; http://iopscience.iop.org/cpb

What follows is a list of articles you may be interested in

High-order Hamiltonian obtained by Foldy-Wouthuysen transformation up to the order of $m\alpha^8$

Tong Chen(陈彤), Xuesong Mei(梅雪松), Wanping Zhou(周挽平), and Haoxue Qiao(乔豪学)
Chin. Phys. B, 2023, 32 (**8**): 083101. DOI: 10.1088/1674-1056/ac9e98

Transition parameters of Li-like ions (Z=7-11) in dense plasmas

Xiang-Fu Li(李向富), Li-Ping Jia(贾利平), Hong-Bin Wang(王宏斌), and Gang Jiang(蒋刚)
Chin. Phys. B, 2021, 30 (**5**): 053102. DOI: 10.1088/1674-1056/abea80

Influence of a strong magnetic field on the hydrogen molecular ion using B-spline-type basis-sets

Zhang Yue-Xia (张月霞), Zhang Xiao-Long (张小龙)
Chin. Phys. B, 2015, 24 (**12**): 123101. DOI: 10.1088/1674-1056/24/12/123101

The geometry structures and electronic properties of Li_mB_n (m+n=12) clusters

Ruan Wen (阮文), Xie An-Dong (谢安东), Wu Dong-Lan (伍冬兰), Luo Wen-Lang (罗文浪), Yu Xiao-Guang (余晓光)
Chin. Phys. B, 2014, 23 (**3**): 033101. DOI: 10.1088/1674-1056/23/3/033101

Molecular properties and potential energy function model of BH under external electric field

Wu Dong-Lan (伍冬兰), Tan Bin (谭彬), Wan Hui-Jun (万慧军), Zhang Xin-Qin (张新琴), Xie An-Dong (谢安东)
Chin. Phys. B, 2013, 22 (**12**): 123101. DOI: 10.1088/1674-1056/22/12/123101

Geometric properties of the first singlet S-wave excited state of two-electron atoms near the critical nuclear charge

Tong Chen(陈彤)[1], Sanjiang Yang(杨三江)[2,†], Wanping Zhou(周挽平)[3], Xuesong Mei(梅雪松)[4], and Haoxue Qiao(乔豪学)[1,‡]

[1] *School of Physics and Technology, Wuhan University, Wuhan* 430072, *China*
[2] *College of Physics and Electronic Science, Hubei Normal University, Huangshi* 435002, *China*
[3] *School of Physics and Telecommunications, Huanggang Normal University, Huanggang* 438000, *China*
[4] *Wuhan Maritime Communication Research Institute, Wuhan* 430072, *China*

(Received 26 May 2024; revised manuscript received 12 July 2024; accepted manuscript online 17 July 2024)

The geometric structure parameters and radial density distribution of $1s2s\,^1S$ excited state of the two-electron atomic system near the critical nuclear charge Z_c were calculated in detail under tripled Hylleraas basis set. Contrary to the localized behavior observed in the ground and the doubly excited $2p^2\,^3P^e$ states, for this state our results identify that while the behavior of the inner electron increasingly resembles that of a hydrogen-like atomic system, the outer electron in the excited state exhibits diffused hydrogen-like character and becomes perpendicular to the inner electron as nuclear charge Z approaches Z_c. This study provides insights into the electronic structure and stability of the two-electron system in the vicinity of the critical nuclear charge.

Keywords: critical nuclear charge, two-electron atomic system, geometric structure, density distribution

PACS: 31.15.ac, 31.15.ae, 31.15.vj **DOI:** 10.1088/1674-1056/ad6422

1. Introduction

The concept of critical nuclear charge Z_c in multi-electron atomic or molecular systems has garnered significant attention in recent years, where Z_c is defined as the minimal nuclear charge necessary to maintain a bound state. With nuclear charge Z approaching Z_c the ionization energy of system, $E_{\rm ion}(Z) = E_e(Z) - E_{2e}(Z)$, gradually decrease to zero. The study of this asymptotic behavior of atomic systems near Z_c plays an important role in understanding quantum phase transitions and symmetry breaking of electron configurations.[1–4] Over the past few decades, lots of researches focus on determining the critical nuclear charge in the two-electron system. For example, based on an extensive variational perturbation calculation with the $1/Z$ expansion, Baker *et al*. estimated $Z_c = 0.91103$ for the ground state.[5] Ivanov later refined this value to 0.91102826 by using a fitting procedure.[6] Deviate from this result, Zamastil *et al*.[7] estimated at $Z_c = 0.9021$ and Guevara and Turbiner's calculation provided that $Z_c = 0.910850$.[8] This discrepancy was resolved by a more precise determination that $Z_c = 0.91102822407725573$ obtained by Estienne *et al*. using Hylleraas basis.[3] Notably, Karr first explored the behavior of resonances when Z is smaller than the critical charge,[9] while Jiao *et al*. further indicated the existence of positive-energy resonances for even smaller nuclear charges.[10] Besides the ground state Yan and Ho investigated the critical nuclear charge for the $2p^2\ ^3P^e$ state, yielding a value of $Z_c = 0.9947812922403662463(1)$.[11] The three-electron atomic system was also computed by Guevara and Turbiner, who obtained a value of $Z_{c,3e} = 2.0090$ for the ground state.[8]

Apart from the specific value of the critical nuclear charge, the characteristics emerging in this vicinity also attract many researcher's attention. For example, Katriel, Puchalski, and Pachucki studied the quantum defect and binding energy for the singly excited $1s2s\,^{1,3}S$ states of the helium isoelectronic sequence in the vicinity of the critical nuclear charge,[12] specifically $Z_c = 1$, as determined by the Simon–Zhislin–Hunziker (SZH) theorem.[13–15] Estienne *et al*. showed that for the ground state as Z transitions from above to below the critical value, previously bound outer electron, instead of escaping the atomic nucleus, undergo a phase transition into a state known as the shape resonance.[3] A similar occurrence of shape resonances is observed in the $2p^2\,^3P^e$ state, where Yan and Ho further explored the variation of resonance energy and width for nuclear charges in the $0.5 < Z < Z_c$ region using the complex scaling method.[11] In the vicinity of Z_c the geometric properties could offer insights into the system's stability.[16] For the doubly excited $2p^2\,^3P^e$ states of two-electron systems Zheng *et al*. calculated geometric quantities and electronic probability density distributions near critical nuclear charge, and then analyzed the stability and behavior in detail.[17] Montgomery *et al*. analyzed the asymp-

†Corresponding author. E-mail: sjyang@hbnu.edu.cn
‡Corresponding author. E-mail: qhx@whu.edu.cn

© 2024 Chinese Physical Society and IOP Publishing Ltd

totic behavior by calculating $\langle r_{12}^k \rangle$ near the critical nuclear charge for the single excited state $1sns\,^{1,3}\mathrm{S}$ of two-electron atomic systems.[18] In contrast to the confinement behavior for the ground and the $2\mathrm{p}^2\,^3\mathrm{P}^\mathrm{e}$ states, their results suggest that as $Z \to 1$, the 1s electron behaves like a hydrogen-like system, while the ns electron tends to a hydrogen-like system with effective charge $(Z-1)$. In this work we focus on the property emerging in the vicinity of Z_c for the $1\mathrm{s}2\mathrm{s}\,^1\mathrm{S}$ state of the two-electron system, performing a careful calculation on the geometric quantities and electron probability density distributions for this state. Our results demonstrate that, as Z approaches Z_c, the outer electron undergoes diffusion, exhibiting a hydrogen-like character and becoming perpendicular to the inner electron.

The arrangement of this paper is as follows. In Section 2 we introduce the construction of the Hylleraas basis with triple-fold nonlinear parameters, along with a computational methodology for calculating geometric quantities and radial density distribution for analyzing the behavior of the inner and outer electrons. In Section 3 we localized Z_c by performing a direct calculation on $E_\mathrm{ion}(Z)$. In the vicinity of Z_c, the geometric quantities and electron probability density distributions are carefully calculated. The relevant results and discussions are presented in this section. Finally, in Section 4, a brief summary is made. Atomic units (a.u.) are used throughout this paper.

2. Method

2.1. Hylleraas basis set

The nonrelativistic Hamiltonian of a two-electron system in center-of-mass frame has the following form:

$$H = -\frac{1}{2\mu_1}\nabla_1{}^2 - \frac{1}{2\mu_2}\nabla_2{}^2 - \frac{1}{2M}\nabla_1\cdot\nabla_2 + \frac{Z}{r_1}+\frac{Z}{r_2}+\frac{1}{r_{12}},$$

where r_i denote the radial distance of the i-th electron from the center of mass, and r_{12} is the distance between the two electrons. μ and M is the reduced mass of electrons and mass of nucleus. In this article, nucleus mass is considered to be infinite.

For a given total angular quantum number L, the trial wave function $\Psi(\boldsymbol{r}_1,\boldsymbol{r}_2)$ could be expanded in terms of the Hylleraas basis

$$\Phi_i(\boldsymbol{r}_1,\boldsymbol{r}_2) = {r_1}^{a_i}{r_2}^{b_i}{r_{12}}^{c_i}\,\mathrm{e}^{-\alpha_\mathrm{p} r_1-\beta_\mathrm{p} r_2}\Lambda^{LM}_{l_1l_2}(\hat{r}_1,\hat{r}_2) \pm (\text{exchange}) \tag{1}$$

with

$$\Lambda^{LM}_{l_1l_2}(\hat{r}_1,\hat{r}_2) = \sum_{m_1m_2}\langle l_1m_1l_2m_2|L_iM_i\rangle \times \mathrm{Y}_{l_1m_1}(\hat{r}_1)\,\mathrm{Y}_{l_2m_2}(\hat{r}_2), \tag{2}$$

where $\mathrm{Y}_{l_im_i}$ is spherical harmonics function, and $\langle l_1m_1l_2m_2|LM\rangle$ is Clebsch–Gordan coefficient. $\hat{r}_i$ is the unit vector of $\boldsymbol{r}_i$, which contains only angular information. N is determined by the input parameter Ω, satisfying $a+b+c\le\Omega$, representing the size of the basis set. Additionally, the subscript p indicates the p-th fold of nonlinear parameters $(\alpha_\mathrm{p},\beta_\mathrm{p})$. In calculation the optimization of nonlinear parameters is necessary. In this work we employ triple sets of nonlinear parameters, namely $\{\alpha_1,\beta_1\}$, $\{\alpha_2,\beta_2\}$, and $\{\alpha_3,\beta_3\}$, which were first utilized in two-electron atoms by Drake.[19] With the constructed the basis set, the energy levels and corresponding wavefunctions are obtained by solving the generalized problem

$$\hat{H}C = E\hat{O}C, \tag{3}$$

where $\hat{H}$ is the hamiltonian matrix with matrix elements $\hat{H}_{ij} = \langle\Phi_i|H|\Phi_j\rangle$ and $\hat{O}$ is the overlapping matrix with matrix element $\hat{O}_{ij} = \langle\Phi_i|\Phi_j\rangle$. The solutions also depend on nonlinear parameters. The calculation of matrix elements for each matrix ultimately comes down to calculating the fundamental integral:

$$I(a,b,c,\alpha,\beta) = \int \mathrm{d}\boldsymbol{r}_1\,\mathrm{d}\boldsymbol{r}_2 {r_1}^a{r_2}^b{r_{12}}^c\,\mathrm{e}^{-\alpha r_1-\beta r_2} \times \Lambda^{*L_iM_i}_{l_1il_{2i}}(\hat{r}_1,\hat{r}_2)\Lambda^{L_jM_j}_{l_{1j}l_{2j}}(\hat{r}_1,\hat{r}_2), \tag{4}$$

where the subscripts i and j refer to the indices of the bra vector and ket vector of the wave function, respectively. We know that r_{12} contains both radial and angular information, which can be expanded as follows:

$$r_{12}^\mathrm{c} = \sum_{l=0}^{p}\mathrm{P}_l(\cos\theta_{12})\sum_{k=0}^{q}C_{clk}{r_<}^{l+2k}{r_>}^{c-l-2k}, \tag{5}$$

among them, $r_>$ and $r_<$ are defined as the larger and smaller values of the radial coordinates r_1 and r_2 of the two electrons, respectively, i.e., $r_> = \mathrm{Max}\,(r_1,r_2)$, $r_< = \mathrm{Min}\,(r_1,r_2)$. $\mathrm{P}_l(\cos\theta_{12})$ is the Legendre function, where θ_{12} represents the angle between the two electrons. The upper limits p and q of the summation satisfy the following relationship:

$$\begin{cases} p=\infty,\ \ q=\frac{1}{2}(c+1), & \text{if } c \text{ is odd},\\ p=\frac{1}{2}c,\ \ q=\frac{1}{2}c-l, & \text{if } c \text{ is even}. \end{cases} \tag{6}$$

The exact expression for the coefficient C_{clk} is

$$C_{clk} = \frac{2l+1}{c+2}\binom{c+2}{2k+1}\prod_{t=0}^{S_{lc}}\frac{2k+2t-c}{2k+2l-2t+1}, \tag{7}$$

where $S_{lc} = \mathrm{Min}\,[l-1, 1/2\,(c+1)]$.

And thus the entire fundamental integral can be separated into radial (I_R) and angular (I_A) parts

$$
\begin{aligned}
I &= \sum_{l=0}^{p}\sum_{k=0}^{q} C_{clk}\int {r_1}^a {r_2}^b {r_<}^{l+2k} {r_>}^{c-l-2k}\,\mathrm{e}^{-\alpha r_1-\beta r_2}\mathrm{P}_l\left(\cos\theta_{12}\right)\Lambda^{*L_iM_i}_{l_{1i}l_{2i}}\left(\hat{r}_1,\hat{r}_2\right)\Lambda^{L_jM_j}_{l_{1j}l_{2j}}\left(\hat{r}_1,\hat{r}_2\right)\mathrm{d}\boldsymbol{r}_1\,\mathrm{d}\boldsymbol{r}_2\\
&= \sum_{l,k} C_{clk}\int {r_1}^{a+2} {r_2}^{b+2} {r_<}^{l+2k} {r_>}^{c-l-2k}\,\mathrm{e}^{-\alpha r_1-\beta r_2}\,\mathrm{d}r_1\,\mathrm{d}r_2\int \mathrm{P}_l\left(\cos\theta_{12}\right)\Lambda^{*L_iM_i}_{l_{1i}l_{2i}}\left(\hat{r}_1,\hat{r}_2\right)\Lambda^{L_jM_j}_{l_{1j}l_{2j}}\left(\hat{r}_1,\hat{r}_2\right)\mathrm{d}\hat{r}_2\,\mathrm{d}\hat{r}_1\\
&= \sum_{l,k} C_{clk} I_{\mathrm{R}}\left(a,b,c,\alpha,\beta,l,k\right) I_{\mathrm{A}}\left(l_{1i},l_{1j},l_{2i},l_{2j},l\right),
\end{aligned}
\tag{8}
$$

every integral in the formula above is an integral over the whole space. The results of radial and angular integrals were introduced in detail in Yan's work,[20] and we give the results directly here

$$
\begin{aligned}
I_{\mathrm{R}}\left(a,b,c,\alpha,\beta,l,k\right) &= \frac{\Gamma\left(a+b+c+6\right)}{\left(\alpha+\beta\right)^{a+b+c+6}}\left[\frac{1}{b+l+2k+3}\,{}_2\mathrm{F}_1\left(1;a+b+c+6;b+4+l+2k;\frac{\beta}{\alpha+\beta}\right)\right.\\
&\quad\left.+\frac{1}{a+l+2k+3}\,{}_2\mathrm{F}_1\left(1;b+c+a+6;a+l+2k+4;\frac{\alpha}{\alpha+\beta}\right)\right],\\
I_{\mathrm{A}}\left(l_{1i},l_{1j},l_{2i},l_{2j},l\right) &= (-1)^{L_i+l_{1i}}\left(l_{1i},l_{1j},l_{2i},l_{2j},l\right)^{1/2}\delta_{L_iL_j}\delta_{M_iM_j}\begin{pmatrix} l_{1j} & l_{1i} & l\\ 0 & 0 & 0\end{pmatrix}\begin{pmatrix} l_{2j} & l_{2i} & l\\ 0 & 0 & 0\end{pmatrix}\begin{Bmatrix} L_i & l_{1i} & l_{2i}\\ l & l_{2j} & l_{1j}\end{Bmatrix},
\end{aligned}
\tag{9}
$$

where Γ is Gamma function, and ${}_2\mathrm{F}_1$ is hypergeometric function. The convention adopted identifies the ordered set $(x,y,z,\ldots)$ with the product $(2x+1)(2y+1)(2z+1)\cdots$. Two matrices $\hat{O}$ and $\hat{H}$ are thus constructed. By substituting them into Eq. (3), according to the variational principle, we utilize Newton's method to optimize the nonlinear parameters $(\alpha_{\mathrm{p}},\beta_{\mathrm{p}})$. Consequently, the coefficient list C of the required wave function and the corresponding energy eigenvalue E can be obtained.

2.2. Geometric quantity calculation

The radial quantities $\langle r_>\rangle$ and $\langle r_<\rangle$ represent the average distance between the outer or inner electrons from nucleus respectively, which are calculated as follows:

$$
\langle r_>\rangle = \langle \min\left(r_1,r_2\right)\rangle, \tag{10}
$$

$$
\langle r_<\rangle = \langle \max\left(r_1,r_2\right)\rangle. \tag{11}
$$

With this definition

$$
\langle r\rangle = \frac{\langle r_>\rangle + \langle r_<\rangle}{2}, \tag{12}
$$

where $\langle r\rangle$ describes the average distance between electron from nucleus. In the calculation of matrix elements for radial geometric quantities, we only need to adjust the radial part of the basic integral, while the angular part remains unchanged. The opposite is true when calculating matrix elements for angular geometric quantities.

Angular geometric quantities $\langle\cos\theta_{12}\rangle$ could be calculated by the following way:

$$
\langle\cos\theta_{12}\rangle = \left\langle\frac{{r_1}^2+{r_2}^2-r_{12}^2}{2r_1r_2}\right\rangle. \tag{13}
$$

The expectation value $\langle\theta_{12}\rangle$ can be expanded into a Legendre polynomial of $\cos\theta_{12}$,[21,22]

$$
\langle\theta_{12}\rangle = \frac{1}{2}\sum_{k=0}^{\infty}\left(2k+1\right)I_kq_k, \tag{14}
$$

where

$$
\begin{aligned}
I_k &= \int_0^{\pi}\mathrm{d}\theta_{12}\sin\theta_{12}\mathrm{P}_k\left(\cos\theta_{12}\right)\theta_{12}\\
&= \int_{-1}^{1}\mathrm{d}x\,\mathrm{P}_k\left(x\right)\arccos\left(x\right),\\
q_k &= \langle\mathrm{P}_k\left(\cos\theta_{12}\right)\rangle.
\end{aligned}
\tag{15}
$$

The expansion coefficient I_k can be performed analytically by the following way:

$$
I_k = \begin{cases}\pi\delta_{k/2,0}, & k=2m,\\ \pi\sum_{i=0}^{m}\frac{(2m+2i+1)!!}{(2i+2)!(2m-2i)!!}\left[\frac{(2i+1)!!}{(2i+2)!!}-1\right], & k=2m+1.\end{cases} \tag{16}
$$

The calculation of $\langle\mathrm{P}_k\left(\cos\theta_{12}\right)\rangle$ can be dealt with the help of

$$
\mathrm{P}_k\left(\cos\theta_{12}\right) = \frac{4\pi}{2k+1}\sum_{m=-k}^{k}\mathrm{Y}^*{}_{km}\left(\hat{r}_1\right)\mathrm{Y}_{km}\left(\hat{r}_2\right). \tag{17}
$$

By applying graph theory to simplify the angular momentum coupling, we can subsequently obtain the integral of the angular part of q_k

$$
\begin{aligned}
G_{q_k} &= \left(l_{1i},l_{1j},l_{2i},l_{2j}\right)\sum_{T_1,T_2}\left(T_1,T_2\right)\begin{pmatrix} k & l_{1i} & T_1\\ 0 & 0 & 0\end{pmatrix}\\
&\quad\times\begin{pmatrix} k & l_{2i} & T_2\\ 0 & 0 & 0\end{pmatrix}\begin{pmatrix} l_{1j} & T_1 & l\\ 0 & 0 & 0\end{pmatrix}\begin{pmatrix} l_{2j} & T_2 & l\\ 0 & 0 & 0\end{pmatrix}\\
&\quad\times\begin{Bmatrix} T_2 & l_{2i} & k\\ l_{1i} & T_1 & L_i\end{Bmatrix}\begin{Bmatrix} l_{2j} & T_2 & l\\ T_1 & l_{1j} & L_i\end{Bmatrix}\delta_{L_iL_j}\delta_{M_iM_j},
\end{aligned}
\tag{18}
$$

where the variables T_1 and T_2 take values within the ranges $|l_{1i}-k|\leqslant T_1\leqslant|l_{1i}+k|$ and $|l_{2i}-k|\leqslant T_2\leqslant|l_{2i}+k|$, respectively.

2.3. Radial density distribution

The radial density distribution function, which describes the probability of finding an electron at a given distance from the nucleus, is helpful to understand the spatial distribution

of electrons in an atomic system. For a two-electron system, the single-electron density distribution function is defined as follows:[17,23]

$$\rho(r) = r^2 \int \mathrm{d}\hat{r} \int \mathrm{d}\boldsymbol{r}_2 \left|\Psi(\boldsymbol{r},\boldsymbol{r}_2)\right|^2 \tag{19}$$

with the normalization condition

$$\int_0^{+\infty} \mathrm{d}r\rho(r) = 1. \tag{20}$$

To describe the radial probability distribution of two electrons, we could divide the probability density distribution function into inner and outer electrons, representing those nearer and farther from the nucleus, respectively. The inner and outer electron distribution can be obtained by

$$\rho_<(r) = \int_r^{+\infty} \mathrm{d}r_2\rho(r,r_2), \quad \rho_>(r) = \int_r^{+\infty} \mathrm{d}r_2\rho(r,r_2), \tag{21}$$

where $\rho(r_1,r_2)$ is the two-electron radial density function, which is defined by the following expression:

$$\rho(r_1,r_2) = {r_1}^2{r_2}^2 \int \mathrm{d}\hat{r}_1\,\mathrm{d}\hat{r}_2 \left|\Psi(\boldsymbol{r}_1,\boldsymbol{r}_2)\right|^2. \tag{22}$$

Similar to Eq. (20), the normalization condition of the inner and outer electron distributions is

$$\int_0^{\infty} \mathrm{d}r\rho_<(r) = \int_0^{\infty} \mathrm{d}r\rho_>(r) = 1. \tag{23}$$

As the radial probability density distribution is angle-independent, rewriting the radial integral suffices for deriving the matrix elements. Their radial integrals have the following form:

$$\begin{aligned}
&I_{\mathrm{R}}^{\rho_>}(r;a,b,c,\alpha,\beta,l,k) \\
&= \mathrm{e}^{-\beta r}\alpha^{-2k-l-a-3}r^{-2k-l+b+c+2}\big(\Gamma(2k+l+a+3) \\
&\quad -\Gamma(2k+l+a+3,\alpha r)\big) \\
&\quad + \mathrm{e}^{-\alpha r}\beta^{-2k-l-b-3}r^{-2k-l+a+c+2}\big(\Gamma(2k+l+b+3) \\
&\quad -\Gamma(2k+l+b+3,\beta r)\big), \\
&I_{\mathrm{R}}^{\rho_<}(r;a,b,c,\alpha,\beta,l,k) \\
&= \mathrm{e}^{-\beta r}r^{2k+l+b+2}\alpha^{2k+l-a-c-3}\Gamma(-2k-l+a+c+3,\alpha r) \\
&\quad + \mathrm{e}^{-\alpha r}r^{2k+l+a+2}\beta^{2k+l-(b+c)-3} \\
&\quad \times\Gamma(-2k-l+b+c+3,\beta r).
\end{aligned} \tag{24}$$

By combining Eqs. (19) and (21), the relationship between these three density distributions could be derived

$$\rho_<(r) + \rho_>(r) = 2\rho(r). \tag{25}$$

3. Result

3.1. Geometric quantity

The non-relativistic energy eigenvalues of the isoelectronic sequence for the singly excited state $1s2s\,{}^1\mathrm{S}$ of the two-electron system, where Z varies continuously in the range $1 < Z \leqslant 2$, are presented in Table 1. In the vicinity of Z_c the system becomes unstable, which makes the calculations more challenging. In our calculations Ω is taken to be 15, with the total number of terms being 1332. Our results are in close agreement with previous works,[12] affirming their accuracy and reliability. The second and third columns of the Table 1 present the energies $E(Z)$ and ionization energies $E_{\mathrm{ion}}(Z)$, respectively, for given values of Z. It can be observed that as Z gradually decreases to 1, the ionization energy rapidly diminishes and tends towards zero.

Table 1. The $1s2s\,{}^1\mathrm{S}$ state energies for the two-electron systems at some selected values of nuclear charge Z calculated by using the tripled Hylleraas basis set.

Z	$E(Z)$	$E_{\mathrm{ion}}(Z)$	$E_{\mathrm{ion}}(Z)$ from Ref. [12]
2	–2.145 974 046 054 417	0.145 974 046 054 417 4	0.145 974 0
1.9	–1.925 128 645 785 298	0.120 128 645 785 298 3	
1.8	–1.716 753 258 589 714	0.096 753 258 589 713 5	
1.7	–1.520 844 574 720 947	0.075 844 574 720 947 4	
1.6	–1.337 399 943 190 835	0.057 399 943 190 835 3	
1.5	–1.166 418 750 893 442	0.041 418 750 893 441 9	0.041 418 75
1.4	–1.007 905 513 986 700	0.027 905 513 986 699 7	
1.3	–0.861 877 123 695 153 6	0.016 877 123 695 153 6	
1.2	–0.728 381 595 672 145 9	0.008 381 595 672 145 9	0.008 381 60
1.1	–0.607 557 832 070 740 3	0.002 557 832 070 740 3	0.002 557 89
1.05	–0.552 023 081 367 882 8	0.000 773 081 367 882 8	0.000 773 081
1.03	–0.530 764 404 441 071 6	0.000 314 404 441 071 6	
1.01	–0.510 092 281 314 088 1	0.000 042 281 314 088 1	0.000 042 281 3
1.005	–0.505 023 856 993 799 0	0.000 011 356 993 799 0	
1.001	–0.501 000 988 924 422 4	0.000 000 488 924 422 4	
1.00015	–0.500 150 022 460 315 6	0.000 000 011 210 315 6	
1.0001	–0.500 100 009 988 190 2	0.000 000 004 988 190 2	
1.00007	–0.500 070 004 895 933 8	0.000 000 002 445 933 8	
1.00005	–0.500 050 002 498 299 7	0.000 000 001 248 299 7	
1.00003	–0.500 030 000 899 599 1	0.000 000 000 449 599 1	
1.00001	–0.500 010 000 099 988 0	0.000 000 000 049 988 0	

Table 2. The sequence of radial geometric structure parameters of a two-electron atomic system as a function of Z.

Z	$\langle r_< \rangle$	$\langle r_> \rangle$	$\langle r_{12} \rangle$	$\langle 1/r_{12} \rangle$	$\langle r \rangle$
2	0.749 162 71	5.196 959 6	5.269 696 2	0.249 682 65	2.973 061 1
1.9	0.788 189 17	5.688 954 3	5.762 830 9	0.227 329 40	3.238 571 7
1.8	0.831 599 50	6.284 726 0	6.359 477 2	0.205 040 66	3.558 162 7
1.7	0.880 193 74	7.022 043 7	7.097 271 2	0.182 808 31	3.951 118 7
1.6	0.934 980 01	7.960 496 9	8.035 604 8	0.160 609 57	4.447 738 5
1.5	0.997 244 03	9.200 899 3	9.274 986 3	0.138 392 22	5.099 071 6
1.4	1.068 645 4	10.931 157	11.002 826	0.116 042 84	5.999 901 2
1.3	1.151 348 8	13.555 570	13.622 562	0.093 311 23	7.353 459 5
1.2	1.248 195 9	18.176 019	18.234 411	0.069 596 61	9.712 107 3
1.1	1.362 891 9	29.664 696	29.706 712	0.043 099 64	15.513 794
1.05	1.428 342 3	48.857 009	48.884 639	0.026 760 48	25.142 676
1.03	1.456 227 6	71.883 522	71.902 929	0.018 590 46	36.669 875
1.01	1.485 141 8	177.586 00	177.594 17	0.007 907 58	89.535 570
1.005	1.492 536 2	330.323 82	330.328 27	0.004 358 29	165.908 18
1.000 15	1.499 775 0	10 035.406	10 035.406	0.000 149 21	5 018.452 7
1.000 1	1.499 850 0	15 035.516	15 035.517	0.000 099 65	7 518.508 2
1.000 07	1.499 895 0	21 463.504	21 463.504	0.000 069 83	10 732.502
1.000 05	1.499 925 0	30 036.682	30 036.682	0.000 049 90	15 019.091
1.000 03	1.499 961 0	49 697.735	49 697.735	0.000 037 31	24 849.617
1.000 01	1.499 985 0	150 035.97	150 035.97	0.000 010 0	75 018.736

Table 3. The sequence of angular geometric structure parameters of a two-electron atomic system as a function of Z.

Z	$\langle \theta_{12} \rangle$	$\langle \cos\theta_{12} \rangle$	$\langle \cos\theta_{12} \rangle - \cos\langle \theta_{12} \rangle$
2	90.989 350	–0.014 657 04	0.002 609 52
1.9	90.969 664	–0.014 365 40	0.002 557 63
1.8	90.942 498	–0.013 962 93	0.002 486 02
1.7	90.905 946	–0.013 421 42	0.002 389 66
1.6	90.857 486	–0.012 703 49	0.002 261 90
1.5	90.793 679	–0.011 758 21	0.002 093 66
1.4	90.709 665	–0.010 513 55	0.001 872 12
1.3	90.598 266	–0.008 863 20	0.001 578 32
1.2	90.448 437	–0.006 643 51	0.001 183 11
1.1	90.243 479	–0.003 607 09	0.000 642 40
1.05	90.115 746	–0.001 714 76	0.000 305 39
1.03	90.061 928	–0.000 917 46	0.000 163 40
1.01	90.013 074	–0.000 193 69	0.000 034 50
1.005	90.004 273	–0.000 063 30	0.000 011 27
1.000 15	90.000 006	–0.000 000 09	0.000 000 02
1.000 1	90.000 003	–0.000 000 04	$< 10^{-8}$
1.000 07	90.000 001	–0.000 000 02	$< 10^{-8}$
1.000 05	90.000 001	$< -1 \times 10^{-8}$	$< 10^{-8}$
1.000 03	90.000 002	$< -1 \times 10^{-7}$	$< 10^{-8}$
1.000 01	90.000 000	$< -1 \times 10^{-9}$	$< 10^{-10}$

With the energy levels and corresponding wavefunctions, we compute the geometric structural parameters of the system and investigate their variation trends with the nuclear charge Z. The results are listed in Tables 2 and 3. Table 2 presents the specific values of the radial geometric structure parameters for different values of Z. The second and third columns of Table 2 present the values of $\langle r_< \rangle$ and $\langle r_> \rangle$, respectively. It can be observed that as Z gradually decreases, $\langle r_> \rangle$ increases at an extremely rapid rate, indicating a rapid movement of outer electrons away from the nucleus; while $\langle r_< \rangle$ also increases, the magnitude of this increase is limited. This implies that as the binding capacity of the atomic nucleus weakens, both electrons tend to move away from the nucleus, with a particularly notable trend observed for electrons in the 2s orbital. The average distance between the two electrons, $\langle r_{12} \rangle$, is listed in the fourth column of the table. Its rate of change is on the same order of magnitude as that of $\langle r_> \rangle$.

When the outer electron is localized at a large distance from the nucleus, it is safe to neglect the correlation effects between two electrons, and to consider the inner electron and the nucleus as a hydrogen-like system. The deviation could be characterized by $\Delta_< = \langle r \rangle_e - \langle r_< \rangle$, where $\langle r \rangle_e = 3/(2Z)$ is the expected value of the hydrogen-like system. Through our calculation, the deviation does not present a trivial reduction, see Fig. 1. This figure illustrates the curve of $\Delta_<$, plotted as a function of nuclear charge Z. As the value of Z decreases, the trend of $\Delta_<$ exhibits an initial increase, reaching a peak within the region near $Z = 1.4$, followed by a gradual decrease. As Z approaches $Z_c = 1$, $\Delta_<$ converges towards zero.

Table 3 presents the specific values of the angular geometric structure parameters. Angular quantities $\langle \cos\theta_{12} \rangle$ and $\langle \theta_{12} \rangle$ are listed in the second and third column of the table. As Z gradually decreases to Z_c, the expected value of the angle between the two electrons slowly decreases to 90°. Generally speaking, $\langle \cos\theta_{12} \rangle$ and $\cos\langle \theta_{12} \rangle$ are not equivalent. However, due to the two electrons becoming perpendicular to each other when Z approaches Z_c, the difference between $\langle \cos\theta_{12} \rangle$ and $\cos\langle \theta_{12} \rangle$ becomes extremely small.

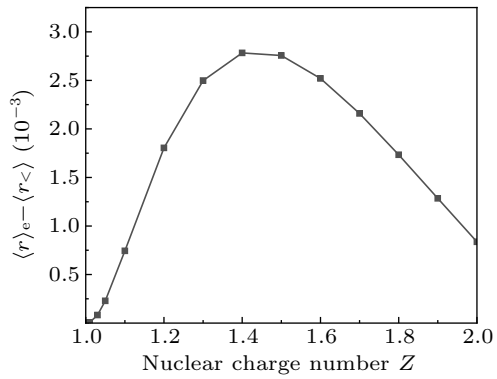


Fig. 1. The difference of inner electron radii between two-electron atomic systems and hydrogen-like atoms with respect to varying nuclear charge Z.

3.2. Electronic density distribution

The probability density distribution of charge approaching to nuclear charge $Z_c = 1$ is presented in two figures. Figure 2 shows the distribution for inner-shell electrons and figure 3 for outer-shell electrons. Table 4 shows the most probable radii and probability densities for various Z-state electron distributions, along with their analogous hydrogen-like system values. For inner-shell electrons, as Z approaches 1, the most probable radius r_p rises while $\rho(r_p)$ decreases. For hydrogen-like atoms with nuclear charge Ze, their radial density distribution can be analytically expressed as $4Z^3r^2e^{-2Zr}$. Compared to hydrogenic atoms, the difference is minimal ($< 10^{-2}$ for $Z = 1.5$) and becomes negligible ($< 10^{-5}$ for $Z = 1.01$). This indicates a strong similarity in inner-shell electron behavior between the $1s2s\,^1S$ state of a two-electron atom and a hydrogen-like atom.

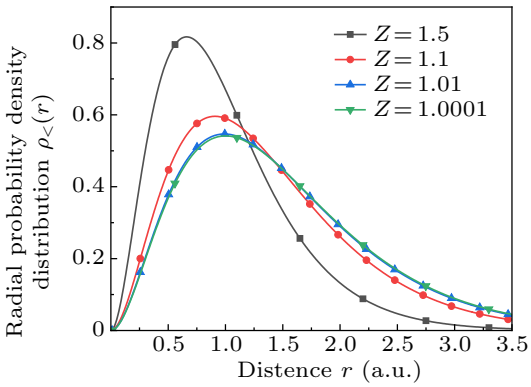


Fig. 2. Probability density distribution of inner-shell electron for various Z.

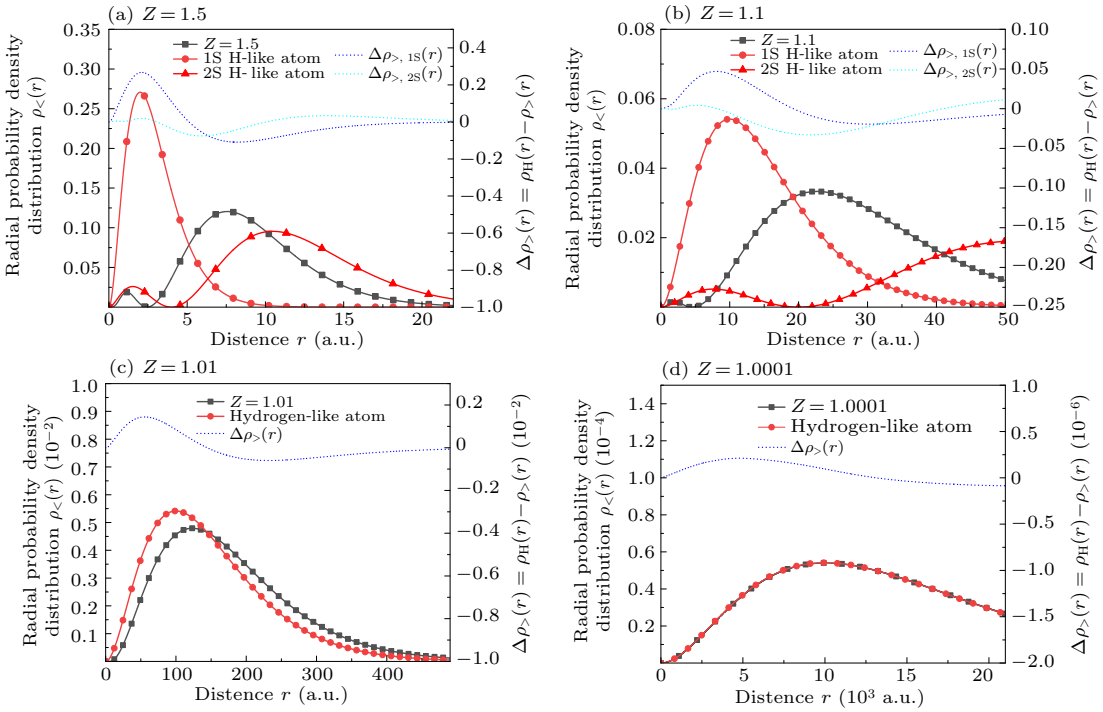


Fig. 3. Probability density distribution of outer-shell electron for various Z.

Figure 3 exhibits the relationship between the radial density distribution of outer electron under four different Z values and the corresponding hydrogen-like atoms with nuclear charge number $(Z-1)$ through four diagrams. The solid black line represents the radial probability distribution of the outer electron in a two-electron atomic system, while the solid red lines, marked with circular and triangular symbols, respectively depict the distributions of 1S and 2S hydrogen-like atoms. The short dashed lines in blue and cyan indicate the probability density differences between those hydrogen-like systems and the two-electron atomic system. When Z is relatively large, such as $Z = 1.5$ (Fig. 3(a)) and $Z = 1.1$ (Fig. 3(b)), the radial probability distribution of the outer electron in the two-electron atomic system exhibits two distinct peaks, a small one and a large one, resembling the distribution characteristics of the 2s orbital of a hydrogen-like atom.

Specifically, for $Z = 1.5$, the target curve lies between the 1S and 2S curves of a hydrogen-like system, resembling the 2S behavior more closely. However, for $Z = 1.1$, the deviation between the target curve and the 2S curve is considerably significant, and the most probable radius is relatively closer to the 1S curve. Furthermore, for even smaller values of Z, specifically at $Z = 1.01$ (Fig. 3(c)) and $Z = 1.0001$ (Fig. 3(d)), the smaller peak on the left attenuates to a barely recognizable level compared to the larger peak on the right. Specifically, the peak value of the smaller peak is 1.77×10^{-5} for $Z = 1.01$ and 4.0×10^{-11} for $Z = 1.0001$. As Z approaches 1, the radial probability distribution of the outer electrons approaches a plane wave-like shape, leading to a rapid increase in the most probable radius and a gradual decrease in the corresponding maximum probability density. Table 4 shows the most probable radii (r_p) and probability density values ($\rho(r_p)$) of a two-electron atomic system for these four Z values. It also compares these values to the 1S and 2S states of a hydrogenic-like system with a nuclear charge of $(Z-1)$.

Table 4. Differences in probability density distributions between two-electron ($1s2s\,^1S$, nuclear charge Z) and hydrogen-like atomic systems.
(a) Inner-electron of two-electron atomic systems and hydrogen-like systems (1s state, nuclear charge (Z)).

Z	r_p	$r_{p,H}$	$\rho(r_p)$	$\rho(r_{p,H})$
1.5	0.661 321 794	0.666 666 667	0.816 901 162	0.812 011 699
1.1	0.908 753 56	0.909 090 909	0.595 920 205	0.595 475 246
1.01	0.990 097 54	0.990 099 01	0.546 757 59	0.546 754 544
1.000 1	0.999 900 01	0.999 900 01	0.541 395 267	0.541 395 267

(b) Outer-electron of two-electron atomic systems and hydrogen-like systems (nuclear charge $(Z-1)$). For each Z, the data for $r_{p,H}$ and $\rho(r_{p,H})$ in the first row corresponds to the 1S state of the hydrogen atom, and the same data in the second row corresponds to the 2S state.

Z	r_p	$r_{p,H}$	$\rho(r_p)$	$\rho(r_{p,H})$
1.5	7.570 446 7	2	0.120 462 24	0.270 670 57
		10.472 135		0.095 483 96
1.1	22.677 373	10	0.033 312 24	0.054 134 11
		52.360 680		0.019 096 79
1.01	123.162 58	100	0.004 792 51	0.005 413 41
		523.606 79		0.001 909 67
1.000 1	10 031.457	10 000	0.000 054 04	0.000 054 13
		52 360.680		0.000 019 10

From the table, it is observable that as Z decreases towards 1, the difference in the most probable radius between the two-electron atomic system and the 2S state of a hydrogenic-like atom rapidly increases, while the difference with the 1S state increases relatively steadily. Moreover, compared to 1S state of hydrogen-like atoms, the outer electrons in the two-electron atomic system exhibit a larger most probable radius and a lower peak probability density. However, despite this significant difference, near $Z = 1$, due to the sufficiently broad distribution of the waveforms, this difference becomes almost negligible in comparison. This can be observed in Fig. 3, where for $Z = 1.0001$, the two waveforms almost overlap with each other.

4. Conclusion

In this work, utilizing tripled Hylleraas basis set, we calculated energy levels and geometric structure parameters for the $1s2s\,^1S$ state of two-electron atomic systems in the vicinity of Z_c. Our results demonstrate the patterns of change in the geometric and distributional properties of the system near the critical nuclear charge. Through radial density distribution we display the diffusion of outer electron, and through $\langle\theta_{12}\rangle$ we show the outer electron becomes perpendicular to the inner electron, as Z approaches Z_c. These results provide a helpful perspective and understanding of the behavior of electrons in atoms under critical conditions, as well as potential insights into similar phenomena in more complex atomic and molecular systems.

Acknowledgement

Project supported by the National Natural Science Foundation of China (Grant Nos. 12074295, 12304271, and 12104420).

References

[1] Hoffmann-Ostenhof M, Hoffmann-Ostenhof T and Simon B 1983 *J. Phys. A: Math. Gen.* **16** 1125
[2] Kais S and Shi Q 2000 *Phys. Rev. A* **62** 060502
[3] Estienne C S, Busuttil M, Moini A and Drake G W F 2014 *Phys. Rev. Lett.* **112** 173001
[4] Kar S, Wang Y S and Ho Y K 2019 *Phys. Rev. A* **99** 042514
[5] Baker J D, Freund D E, Hill R N and Morgan J D 1990 *Phys. Rev. A* **41** 1247
[6] Ivanov I A 1995 *Phys. Rev. A* **51** 1080
[7] Zamastil J, Čížek J, Skála L and Šimánek M 2010 *Phys. Rev. A* **81** 032118
[8] Guevara N L and Turbiner A V 2011 *Phys. Rev. A* **84** 064501
[9] Karr J P 2015 *Phys. Rev. A* **92** 042505
[10] Jiao L G, Zheng R Y, Liu A, Montgomery H E and Ho Y K 2022 *Phys. Rev. A* **105** 052806
[11] Yan Z C and Ho Y K 2015 *J. Phys.: Conf. Ser.* **635** 052015
[12] Katriel J, Puchalski M and Pachucki K 2012 *Phys. Rev. A* **86** 042508
[13] Simon B 1970 *Helvetica Physica Acta* **43** 607
[14] Zhislin G M 1971 *Theor. Math. Phys.* **7** 571
[15] Hunziker W 1975 *Helvetica Physica Acta* **48** 145
[16] Bressanini D 2018 *Phys. Rev. A* **97** 012503
[17] Zheng R Y, Jiao L G, Liu A, Ma J, Jr H E M, Ho Y K and Fritzsche S 2023 *J. Phys.B: At. Mol. Opt. Phys.* **56** 095002
[18] Montgomery H, Katriel J and Sen K 2019 *Phys. Lett. A* **383** 126007
[19] Drake G W F, Cassar M M and Nistor R A 2002 *Phys. Rev. A* **65** 054501
[20] Yan Z C and Drake G W F 1996 *Chem. Phys. Lett.* **259** 96
[21] Koga T 2002 *J. Chem. Phys.* **117** 10493
[22] Jiao L G, Zan L R, Zhu L, Zhang Y Z and Ho Y K 2019 *Phys. Rev. A* **100** 022509
[23] Koga T and Matsuyama H 2006 *Theoretical Chemistry Accounts* **115** 59